Reducing PAPR of SC-FDMA Signals through Simple Amplitude Predistortion

Yujie Xia and Jinwei Ji

A novel peak-to-average power ratio (PAPR) reduction method is proposed for single-carrier frequency-division multiple access (SC-FDMA) signals. The proposed method deliberately distorts the amplitude values of a few of the complex modulated symbols that cause peaks beyond a predetermined threshold in the samples of the output signal. The method then marks the location indices of the distorted symbols by using a pilot block at the transmitter without transmitting side information. At the receiver, the method is then able to recover the distorted amplitude values through the marked location indices. Computer simulation results show that when compared to conventional SC-FDMA signals, the proposed scheme can effectively reduce the PAPR of SC-FDMA signals with asymptotically consistent bit error rate (BER) performance.

Keywords: Peak-to-average power ratio, single-carrier frequency-division multiple access, amplitude predistortion, complementary cumulative distribution function, CCDF, PAPR, SC-FDMA.

I. Introduction

The 3rd Generation Partnership Project's Long-Term Evolution radio standard has adopted a special form of orthogonal frequency-division multiplexing (OFDM) signaling for the uplink of multiple access networks, called single-carrier frequency-division multiple access (SC-FDMA) [1]. SC-FDMA uplink signals fall into two categories — localized SC-FDMA (LFDMA) and interleaved SC-FDMA (IFDMA) — according to the subcarrier mapping scheme used. For modulations of a high order, such as 16 quadrature amplitude modulation (QAM), an LFDMA signal has a much larger peak-to-average power ratio (PAPR) compared to an IFDMA signal [2]–[3]. Therefore, in the case of LFDMA signals, a large back-off of the transmit power amplifier from its output saturation point is required, which leads to very low power efficiency. This problem is particularly serious for the uplink of multiple access networks due to the stringent power consumption demands on user terminals [4]. In this paper, we focus on PAPR reduction for LFDMA uplink signals.

Various schemes based on different theories and hypotheses attempting to reduce the PAPR of OFDM systems have appeared in the literature [5]–[9]. However, those methods are mainly focused on PAPR reduction in relation to specific characteristics of OFDM signals; consequently, such methods are not suitable for SC-FDMA signals. Recently, a number of PAPR reduction schemes for SC-FDMA signals have been proposed, including amplitude clipping [10], selected mapping [11]–[12], and partial transmit sequences [13]–[14]. However, the computational complexity of these methods is high, and a large amount of side information is needed to transmit for correct demodulation at a receiver. References [15]–[17] present a pulse shaping method to reduce the PAPR of SC-

Manuscript received Oct. 6, 2014; revised Jan. 13, 2015; accepted June 1, 2015.

This work was supported in part by the Key Scientific and Technological Project of He'nan Province of China under Grant No. 152102210333 and by the Applied Research Programs of Science and Technology of Luoyang Normal University of China under Grant No. 2014-YYJJ-002.

Yujie Xia (corresponding author, yjxia@mail.xidian.edu.cn) is with the School of Physics and Electronics Information, Luoyang Normal University, China.

Jinwei Ji (jjw86215@163.com) is with the 54th Research Institute of China Electronics Technology Group Corporation, Shijiazhuang, China.

http://dx.doi.org/10.4218/etrij.15.0114.1194

FDMA signals by imposing a linear filtering operation on the outputs of a discrete Fourier transform (DFT) precoder, but the PAPR reduction performance degrades significantly in the case of excess bandwidth. Moreover, it also causes a noise enhancement penalty, which induces a loss in the bit error rate (BER) performance due to the frequency-domain filtering on the transmitted signal. To avoid the high computational load and excess bandwidth, [18] proposes a new scheme with high PAPR reduction performance for coded SC-FDMA signals. However, the BER performance suffers a slight loss through the introduction of a few bit errors.

To improve the PAPR performance and avoid the high computational load, a novel amplitude predistortion–based PAPR reduction scheme is presented for localized SC-FDMA signals, in this paper. In the proposed scheme, the amplitude values of a few of the complex modulated symbols that cause peaks beyond a predetermined threshold are deliberately distorted and the corresponding location indices are marked by using a pilot block at the transmitter. At the receiver, the location indices of the distorted symbols are directly determined by using channel estimation, and the distorted symbols are efficiently recovered without the need for side information.

The rest of this paper is organized as follows. In Section II, the signal models of PAPR for SC-FDMA systems are introduced. In Section III, the reasons behind the occurrence of the aforementioned large peaks are analyzed for SC-FDMA signals. In Section IV, a novel amplitude predistortion–based PAPR reduction scheme is proposed and the corresponding data recovery method at the receiver is presented. The complexity analyses are also shown in this section. In Section V, simulation results are provided in terms of PAPR reduction and BER performances. Finally, brief conclusions are given in Section VI.

II. Signal Models

We consider a typical SC-FDMA uplink system with Z data blocks, each of which transmits M complex modulated symbols. The mth complex modulated block, $\mathbf{s}^{(m)}$ = $[s^{(m)}(0), \ldots, s^{(m)}(n'), \ldots, s^{(m)}(M-1)]^{\mathrm{T}}$, is linearly precoded by an M by M DFT matrix, $\mathbf{F}$, whose element is $e^{-\mathrm{j}2\pi kn'/M}/\sqrt{M}$ for $0 \le n' \le M-1$, $0 \le k \le M-1$; thus, the output data matrix $\mathbf{X}^{(m)}$ of the precoder in the frequency domain can be expressed as

$$\mathbf{X}^{(m)} = \mathbf{F}\mathbf{s}^{(m)}, \tag{1}$$

where $\mathbf{X}^{(m)} = [X^{(m)}(0), \ldots, X^{(m)}(k), \ldots, X^{(m)}(M-1)]^{\mathrm{T}}$ with $X^{(m)}(k) = 1/\sqrt{M}\sum_{n'=0}^{M-1} s^{(m)}(n')e^{-\mathrm{j}\frac{2\pi kn'}{M}}$ for $0 \le k \le M-1$.

For LFDMA signals, the elements of $\mathbf{X}^{(m)}$ are mapped to M contiguous inputs of an N-point ($N > M$) inverse fast Fourier transform (IFFT) block with the indices denoted as $\{f_k | f_k = f_0 + k, 0 \le f_k \le N-1\}$ for $0 \le k \le M-1$. After inserting a cyclic prefix (CP), the nth samples ($0 \le n \le N-1$) of the mth block in the time domain can be expressed as

$$\begin{aligned} x^{(m)}(n) &= \frac{1}{\sqrt{N}}\sum_{k=0}^{M-1} X^{(m)}(k)e^{\mathrm{j}2\pi f_k n/N} \\ &= \frac{1}{\sqrt{M}}e^{\mathrm{j}2\pi f_0 n/N}\sum_{n'=0}^{M-1} s^{(m)}(n')g\left(n - n'\frac{N}{M}\right), \end{aligned} \tag{2}$$

where $g(n)$ is given as

$$g(n) = \frac{1}{\sqrt{N}}e^{\mathrm{j}\pi(M-1)n/N}\sin\frac{\pi Mn}{N}\Big/\sin\frac{\pi n}{N}. \tag{3}$$

The PAPR in (2) is defined as

$$\mathrm{PAPR}(x^{(m)}(n)) = \frac{\max\limits_{0\le n\le N-1}\left|x^{(m)}(n)\right|^2}{\mathrm{E}\left\{\left|x^{(m)}(n)\right|^2\right\}}, \qquad 1 \le m \le Z. \tag{4}$$

At the receiver, after removing CP, the received vector of the mth block is

$$\mathbf{y}^{(m)} = \mathbf{h}^{(m)} \otimes_N \mathbf{x}^{(m)} + \mathbf{w}^{(m)}, \tag{5}$$

where $\mathbf{y}^{(m)} = [y^{(m)}(0), y^{(m)}(1), \ldots, y^{(m)}(N-1)]^{\mathrm{T}}$, $\otimes_N$ denotes the N-point circular convolution operation, $\mathbf{x}^{(m)}$ = $[x^{(m)}(0)$, $x^{(m)}(1), \ldots, x^{(m)}(N-1)]^{\mathrm{T}}$ is the transmitted vector of the mth block in the time domain, $\mathbf{h}^{(m)} = \left[h^{(m)}(0), h^{(m)}(1), \ldots,\right.$ $\left.h^{(m)}(L-1)\right]^{\mathrm{T}}$ is the time-domain impulse response of the channel over the mth SC-FDMA block, L is the total number of resolvable multipaths, and $\mathbf{w}^{(m)}$ = $[w^{(m)}(0), w^{(m)}(1), \ldots, w^{(m)}(N-1)]^{\mathrm{T}}$ represents an additive white Gaussian noise (AWGN) vector. After an N-point fast Fourier transform (FFT) of $\mathbf{y}^{(m)}$, the received symbol of the mth block at the f_kth subcarrier is

$$Y^{(m)}(f_k) = H^{(m)}(f_k)X^{(m)}(k) + W^{(m)}(f_k), \tag{6}$$

where $W^{(m)}(f_k)$ represents the AWGN noise component and $H^{(m)}(f_k)$ is the impulse response of a wireless channel in the frequency domain with $H^{(m)}(f_k) = \sum_{l=0}^{L-1} h^{(m)}(l)e^{-\mathrm{j}\frac{2\pi f_k l}{N}}$.

III. Occurrence of Large Peaks for SC-FDMA Signals

From (2), the conventional SC-FDMA signals can be seen as a combination of a complex modulated symbol and a weighted factor. From the expression for $g(n)$ in (3), it can be seen that the signal samples of two successive pulses $g(n - dN/M)$ and $g(n - (d+1)N/M)$ at their intersection point differ in phase by

$$\frac{(M-1)\pi}{M} \approx \pi. \tag{7}$$

To gain further insight into the peaks of SC-FDMA signals, we rewrite (2) as follows:

$$\begin{aligned} x^{(m)}(n) = \frac{e^{j2\pi f_0 n/N}}{\sqrt{M}} \Bigg\{ & s^{(m)}(d) g\left(n - d\frac{N}{M}\right) \\ & + s^{(m)}(d+1) g\left(n-(d+1)\frac{N}{M}\right) \\ & + \sum_{\substack{n'=0 \\ n'\neq d \\ n'\neq d+1}}^{M-1} s^{(m)}(n') g\left(n - n'\frac{N}{M}\right) \Bigg\}. \end{aligned} \tag{8}$$

For high-order modulations (for example, 16-QAM), peaks of SC-FDMA signals will always occur when two successive complex modulated symbols in one SC-FDMA block are the outermost constellation points and differ in phase by nearly π radians.

IV. Proposed PAPR Reduction Scheme

In this section, we propose a novel amplitude predistortion–based PAPR scheme for SC-FDMA signals. To further reduce the PAPR of SC-FDMA signals, we also propose an iterative predistortion scheme. Then, a distorted symbols recovery scheme is illustrated at the receiver. Finally, we analyze the computational complexity of the two proposed schemes.

1. Proposed Amplitude Predistortion Scheme

From (4), we can evaluate the PAPR of the output samples $x^{(m)}(n),\ 0 \le n \le N-1,$ of the mth block and determine the maximum PAPR as

$$n_{\max} = \arg\max_{n\in[0,N-1]} \{\mathrm{PAPR}(x^{(m)}(n))\}, \tag{9}$$

where $n_{\max}$ is the location of the output sample with the maximum PAPR for the mth block.

The peak value occurs around the intersection of the main lobes of two successive pulses, $g(n-dN/M)$ and $g(n-(d+1)N/M)$; the indices of the two pulses can be determined as

$$n' = \lfloor n_{\max} / (N/M) \rfloor, \tag{10}$$

$$n'+1 = \lfloor n_{\max} / (N/M) \rfloor + 1, \tag{11}$$

where $\lfloor\ \rfloor$ is a truncation operation. For the aforementioned peak value, the modulated symbols of $s^{(m)}(n')$ and $s^{(m)}(n'+1)$ must be the outermost constellation points with phase difference of π. For a given n', if the amplitude of

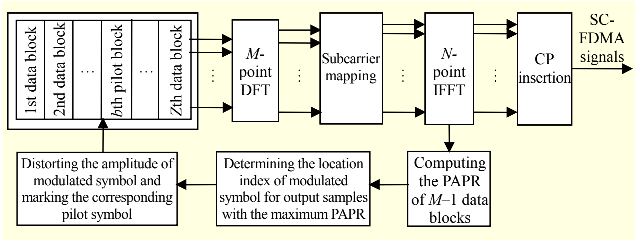

Fig. 1. Block diagram of proposed scheme for PAPR reduction.

$s^{(m)}(n')$ is multiplied by a real factor γ ($|\gamma| < 1$), then it will efficiently reduce the magnitude of the peak value by transmitting $\gamma s^{(m)}(n')$ with amplitude distortion; on the other hand, if the location index of distorted symbol $\gamma s^{(m)}(n')$ is determined, then the corresponding modulated symbols can be easily recovered at the receiver. This means that the PAPR problem of SC-FDMA signals can be reduced by amplitude predistortion. Figure 1 illustrates the key idea of the proposed amplitude predistortion scheme for PAPR reduction of SC-FDMA signals.

In the proposed scheme, the Z modulated blocks are dealt with as a processing unit — one that consist of $Z - 1$ data blocks and one pilot block. Suppose that the bth block $\mathbf{X}^{(b)} = [X^{(b)}(0), X^{(b)}(1), \ldots, X^{(b)}(M-1)]^{\mathrm{T}}$ is the pilot symbol in the frequency domain. Every v symbols in $\mathbf{X}^{(b)}$ are reserved for channel estimation, and the other symbols in $\mathbf{X}^{(b)}$ can be used to indicate the locations of distorted symbols in transmitting blocks. The variable v is selected in such a way so as to be sufficiently small in comparison with the coherent bandwidth of the multipath channels. The indices of the pilot symbols in $\mathbf{X}^{(b)}$, representing either channel estimation or the locations of distorted symbols, are denoted by the sets $\Phi_1 = \{k \mid k \equiv 0 \pmod{v}\}$ and $\Phi_2 = \{k \mid k \neq 0 \pmod{v}\}$, respectively. For all $Z - 1$ data blocks in the processing unit, one can obtain the maximum PAPR of the output samples of SC-FDMA signals $x^{(m)}(n), 0 \le n \le N-1,$ for $1 \le m \le Z,$ $m \neq b;$ the maximum PAPR is determined by

$$\{u, n_{\max}\} = \arg\max_{\substack{m\in[1,Z], \\ m\neq b}} \arg\max_{n\in[0,N-1]} \{\mathrm{PAPR}(x^{(m)}(n))\}, \tag{12}$$

where u and $n_{\max}$ are the index of a data block, and the location index of an output sample of the uth block with a maximum PAPR, respectively.

Therefore, the maximum PAPR of $(Z - 1)N$ output samples for $Z - 1$ transmitting data blocks is $\mathrm{PAPR}(x^{(u)}(n_{\max}))$. If $\mathrm{PAPR}(x^{(u)}(n_{\max})) < A,$ where A is a predetermined threshold, then there are no symbols that can be distorted; otherwise, the indices of n' and $n' + 1$ of a modulated block are calculated by (10) and (11), respectively. When $n' \in \Phi_2$, $\{s^{(u)}(n'),$ $u = 1, 2, \ldots, Z, u \neq b\}$ are all distorted, the pilot symbol

http://dx.doi.org/10.4218/etrij.15.0114.1194

$X^{(b)}(n')$ in $\mathbf{X}^{(b)}$ is marked as $-X^{(b)}(n')$, and the location index of n' is deleted from Φ_2. If $n' \notin \Phi_2$ and $n'+1 \in \Phi_2$, then $\left\{s^{(u)}(n'+1), u=1,2,\ldots,Z, u \neq b\right\}$ are all distorted and the pilot symbol $X^{(b)}(n'+1)$ is marked as $-X^{(b)}(n'+1)$; the location index of $n'+1$ is deleted form Φ_2. When $n' \notin \Phi_2$ and $n'+1 \notin \Phi_2$, the predistortion operation stops.

Let n' be the location index of a distorted symbol. Then, we can rewrite the Z – 1 data blocks as $\mathbf{s}_1^{(u)} = [s^{(u)}(0), s^{(u)}(1), \ldots, \gamma s^{(u)}(n'), \ldots, s^{(u)}(M-1)]^{\mathrm{T}}$ for $u = 1,2,\ldots,Z$, $u \neq b$ and the pilot block as $\mathbf{X}_1^{(b)} = [X^{(b)}(0), X^{(b)}(1), \ldots, -X^{(b)}(n'), \ldots, X^{(b)}(M-1)]^{\mathrm{T}}$. Suppose $\mathbf{x}_1^{(u)} = [x_1^{(u)}(0), x_1^{(u)}(1), \ldots, x_1^{(u)}(N-1)]^{\mathrm{T}}$ for $u = 1,2,\ldots, Z, u \neq b$ and $\mathbf{x}_1^{(b)} = [x_1^{(b)}(0), x_1^{(b)}(1), \ldots, x_1^{(b)}(N-1)]^{\mathrm{T}}$ are the transmitted vector of a data block and that of a pilot block after a predistortion operation in the time domain, respectively. The corresponding transmitted samples can be expressed as

$$x_1^{(u)}(n) = x^{(u)}(n) + \frac{1}{\sqrt{M}} e^{\mathrm{j}2\pi f_0 n/N} \times (\gamma - 1) s^{(u)}(n') g\left(n - n'\frac{N}{M}\right), \tag{13}$$

$$x_1^{(b)}(n) = x^{(b)}(n) - \frac{2}{\sqrt{N}} X^{(b)}(n') e^{\mathrm{j}2\pi f_{n'} n/N}. \tag{14}$$

Note that $\mathbf{X}_1^{(b)}$ carries the location information of distorted symbols in $\mathbf{s}_1^{(u)}$ for u = 1, 2, … , Z, $u \neq b$. By setting a reasonable threshold, A, at most one symbol in each data block is distorted for an SC-FDMA uplink signal.

2. Extension of Predistortion Scheme in Iterative Fashion

To further reduce the PAPR of SC-FDMA signals, we extend the above procedure in iterative fashion. In the proposed method, let K be the number of iterations. Let us assume $\mathbf{x}_{i-1}^{(m)} = [x_{i-1}^{(m)}(0), \ldots, x_{i-1}^{(m)}(n), \ldots, x_{i-1}^{(m)}(N-1)]^{\mathrm{T}}$ and $\mathbf{x}_{i-1}^{(b)} = [x_{i-1}^{(b)}(0), \ldots, x_{i-1}^{(b)}(n), \ldots, x_{i-1}^{(b)}(M-1)]^{\mathrm{T}}$ are the transmitted vectors of the mth data block $(m = 1, 2, \ldots, Z,\ m \neq b)$ and that of the pilot block at iteration i–1. We define a set Ψ_{i-1} whose elements are Φ_2 but without the location indices of the distorted symbols for all i – 1 iterations. At iteration i, one can calculate the PAPR of $x_{i-1}^{(m)}(n), m = 1,2,\ldots,Z, m \neq b$ by using (2) and determine the location index of output sample of corresponding data block $\{u,\ n_{\max}\}$ with a maximum PAPR of $\mathrm{PAPR}(x_{i-1}^{(u)}(n_{\max}))$ by utilizing (12). If $\mathrm{PAPR}(x_{i-1}^{(u)}(n_{\max})) \geq A_i$, where A_i is a threshold at iteration i, then the indices n' and $n'+1$ of the uth block are calculated by (10) and (11), respectively. We let $n' \in \Psi_{i-1}$ be the index of a distorted symbol at iteration i, and we define $\mathbf{s}_i^{(u)} = [s_i^{(u)}(0), \ldots, s_i^{(u)}(n'), \ldots, s_i^{(u)}(M-1)]^{\mathrm{T}}$ with $s_i^{(u)}(n') = \gamma s^{(u)}(n')$ and $\mathbf{X}_i^{(b)} = [X_i^{(b)}(0), \ldots, X_i^{(b)}(n'), \ldots, X_i^{(b)}(M-1)]^{\mathrm{T}}$ with $X_i^{(b)}(n') = -X^{(b)}(n')$. The output samples $x_i^{(u)}(n), 0 \leq n \leq N-1$, of an SC-FDMA signal at iteration i can be expressed as

$$x_i^{(u)}(n) = x_{i-1}^{(u)}(n) + \frac{1}{\sqrt{M}} e^{\mathrm{j}2\pi f_0 n/N} \times (\gamma - 1) s_i^{(u)}(n') g\left(n - n'\frac{N}{M}\right). \tag{15}$$

Obviously, $x_i^{(b)}(n), 0 \leq n \leq N-1$, of $\mathbf{x}_i^{(b)}$ at iteration i is

$$x_i^{(b)}(n) = x_{i-1}^{(b)}(n) - \frac{2}{\sqrt{N}} X_i^{(b)}(n') e^{\mathrm{j}2\pi f_{n'} n/N}. \tag{16}$$

In fact, the iterative procedure stops if $\mathrm{PAPR}(x_{i-1}^{(u)}(n_{\max})) < A_i$ or $n' \notin \Psi_{i-1}$ and $n'+1 \notin \Psi_{i-1}$. The proposed iterative PAPR reduction scheme can be described as follows:

1) Initial the iteration number K and let $\Psi_0 = \Phi_2$, $\mathbf{x}_0^{(m)} = \mathbf{x}^{(m)}$ for $1 \leq m \leq Z$;
2) For i = 1:K
 set a predetermined threshold value A_i;
 calculate the PAPR of SC-FDMA signals by using (4);
 determine the index of peak location of data block with the maximum PAPR by
 $\{u, n_{\max}\} = \arg\max_{m\in[1,Z],\, m\neq b} \arg\max_{n\in[0,N-1]} \{\mathrm{PAPR}(x_{i-1}^{(m)}(n))\}$
 if $\mathrm{PAPR}(x^{(u)}(n_{\max})) \leq A_i$
  break;
 else
  compute the symbol index n' and $n'+1$ by using (10) and (11);
  if $n' \in \Psi_{i-1}$
   $s^{(u)}(n') = \gamma s^{(u)}(n')$,
    $X^{(b)}(n') = -X^{(b)}(n')$,
    $\Psi_i = \Psi_{i-1} - n'$;
   else if $n' \notin \Psi_{i-1}$ & $n'+1 \in \Psi_{i-1}$
   $s^{(u)}(n'+1') = \gamma s^{(u)}(n'+1)$,
    $X^{(b)}(n'+1) = -X^{(b)}(n'+1)$,
    $\Psi_i = \Psi_{i-1} - (n'+1)$;
  else $n' \notin \Psi_{i-1}$ & $n'+1 \notin \Psi_{i-1}$
    stop iteration and break;
   end if
   Use (15) and (16) to compute the updated signals;
  end if
end for

When all K iterations are complete, the nth output sample of the mth data block (m = 1, 2, … , Z, $u \neq b$) and that of the pilot block for SC-FDMA signals are updated as follows:

$$x_K^{(m)}(n) = x^{(m)}(n) + \frac{1}{\sqrt{M}} e^{j2\pi f_0 n/N} \times \sum_{n' \in S_K} (\gamma - 1) s^{(m)}(n') g\left(n - n'\frac{N}{M}\right), \tag{17}$$

$$x_K^{(b)}(n) = x^{(b)}(n) - \frac{2}{\sqrt{N}} \sum_{n' \in S_K} X^{(b)}(n') e^{j2\pi f_{n'} n/N}, \tag{18}$$

where S_K is a set whose elements are the indices of distorted symbols in the processing unit for all K iterations.

3. Distorted Symbols Recovery Scheme at Receiver

At the receiver, since the pilot block $\mathbf{X}^{(b)}$ is known to the receiver and every v symbols of $\mathbf{X}^{(b)}$ in the frequency domain are kept unchanged, the location indices of distorted symbols can be easily obtained by detecting those of the reversed symbols of $\mathbf{X}^{(b)}$. Figure 2 illustrates a block diagram of the distorted symbols recovery scheme at the receiver.

A received pilot symbol after an N-point FFT over the f_kth subcarrier ($k = 0, 1, \ldots, M-1$) is given by

$$Y^{(b)}(k) = H(f_k) X_K^{(b)}(k) + W^{(b)}(f_k). \tag{19}$$

Since $X_K^{(b)}(k) = X^{(b)}(k)$ for $k \in \Phi_1$, the channel frequency response $\hat{H}(f_k)$ for $k \in \Phi_1$ can be obtained as

$$\hat{H}(f_k) = H(f_k) + \frac{W^{(b)}(f_k)}{X^{(b)}(k)}. \tag{20}$$

Since the spacing v between two adjacent unchanged pilot symbols is sufficiently small as compared to the coherent bandwidth of the multipath channels, the channel frequency response $\hat{H}(f_k)$ for $k = 0, 1, \ldots, M-1$ can be obtained by simple liner interpolation. We define a sign vector $\mathbf{p} = [p(0), \ldots, p(k), \ldots, p(M-1)]^{\mathrm{T}}$, for which

$$p(k) = \operatorname{sgn}\left\{\Re\left\{Y^{(b)}(f_k) / \left(\hat{H}(f_k) X^{(b)}(k)\right)\right\}\right\}, \tag{21}$$

where $\Re\{\ \}$ denotes the real part of a complex quantity. Note that the number of $p(k) = -1$ for $k = 0, 1, \ldots, M-1$ in $\mathbf{p}$ is at most K, where K is the number of iterations. We define $\Phi_3 = \{k \mid p(k) = -1,\ k \in [0, M-1]\}$ to be the set of location indices of distorted symbols.

With $\mathbf{p}$, to improve the accuracy of $\hat{H}(f_k)$ for $k = 0, 1, \ldots, M-1$, it can be estimated again as

$$\hat{H}(f_k) = \frac{Y^{(b)}(f_k)}{p(k) X^{(b)}(k)} = H(f_k) + \frac{W^{(b)}(f_k)}{p(k) X^{(b)}(k)}. \tag{22}$$

The received data symbol after an N-point FFT over the f_kth subcarrier ($k = 0, 1, \ldots, M-1$) for $u = 1, 2, \ldots, Z$, $u \neq b$ is given by

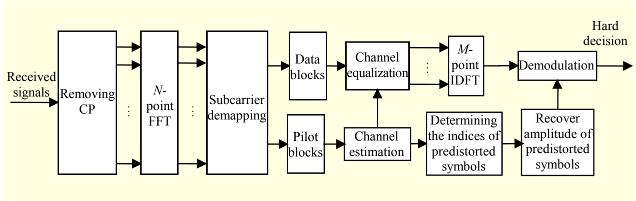

Fig. 2. Block diagram of distorted symbols recovery scheme at receiver.

$$Y^{(u)}(k) = H(f_k) X_K^{(u)}(k) + W^{(u)}(f_k), \tag{23}$$

where $X_K^{(u)}(k) = 1/\sqrt{M} \sum_{n'=0}^{M-1} s_K^{(u)}(n') e^{-j\frac{2\pi k n'}{M}}$ with $s_K^{(u)}(n') = \gamma s^{(u)}(n')$ for $n' \in \Phi_3$ and $s_K^{(u)}(n') = s^{(u)}(n')$ for $n' \notin \Phi_3$. Therefore, the received symbols in the frequency domain of the proposed algorithm can be equalized in the same way as those of a conventional SC-FDMA system. The equalized symbols are transformed back to the time domain via an M by M IDFT decoding matrix, $\mathbf{F}^{\mathrm{H}}$, and the distorted symbols of data blocks can then be recovered by an inverse operation. The demodulated symbol $\hat{s}^{(u)}(n)$ for $n \in \Phi_3$ is given by

$$\begin{aligned} \hat{s}^{(u)}(n) &= \frac{1}{\gamma}\sqrt{M} \sum_{k=0}^{M-1} Y^{(u)}(k) / H(f_k) e^{j\frac{2\pi k n}{M}} \\ &= s^{(u)}(n) + \frac{\sqrt{M}}{\gamma} \sum_{k=0}^{M-1} W^{(u)}(f_k) / H(f_k) e^{j\frac{2\pi k n}{M}}. \end{aligned} \tag{24}$$

Since the amplitudes of the distorted symbols can be recovered at the receiver, it is expected that the BER performance of the proposed scheme will approximately approach that of the conventional SC-FDMA systems when there are no error detections of $\mathbf{p}$.

4. Computational Complexity

Consider that a complex multiplication is equivalent to four real multiplications (RMs) plus two real additions (RAs), a complex addition is translated into two RAs, and $|\,|^2$ represents two RMs and one RA.

At the transmitter, there are at most $(Z-1)N$ $|\,|^2$ operations to compute the power of the output samples of SC-FDMA signals, where $Z-1$ is the number of data blocks and N is the total number of subcarriers of the SC-FDMA systems. For the predistortion operation in (13) and (14), $2(Z-1) + 2ZN\log_2 N$ RMs and $ZN\log_2 N$ RAs are needed for Z modulated blocks. Compared to the conventional SC-FDMA signals without PAPR procedure, the additional complexity for the proposed scheme without iteration is about $2(Z-1)(N+1) + 2ZN\log_2 N$ RMs and $(Z+1)N + ZN\log_2 N$ RAs. For the proposed iterative scheme, the additional complexity for PAPR reduction can be represented as the product of the number of iterations K and the

http://dx.doi.org/10.4218/etrij.15.0114.1194

Table 1. Computational complexity comparison of two proposed schemes.

Algorithm	Number of RMs	Number of RAs
Proposed scheme for $K = 1$	$2(Z-1)(N+1) + 2ZN\log_2 N$	$(Z+1)N + ZN\log_2 N$
Proposed Iterative scheme for $K > 1$	$2(Z-1)(N+1)K + 2KZN\log_2 N$	$(Z+1)KN+ZKN\log_2 N$

number of RMs and RAs needed at each iteration.

At the receiver, with channel equalization and demodulation modules of an SC-FDMA system, the location indices can be directly obtained and the distorted symbols can be recovered with a very low additional complexity. So, the additional complexity of the proposed method can be negligible at the receiver.

Table 1 shows a comparison of the computational complexity for the two proposed schemes for PAPR reduction. From the results in Table 1, it can be seen that the complexity of the proposed iterative scheme is about K-times more than that of the predistortion scheme without iteration. Note that the exact complexity of the proposed iterative method depends on the number of iterations.

V. Simulation Results

PAPR reduction performances of the conventional and proposed schemes of localized SC-FDMA uplink signals were investigated by computer simulations. The SC-FDMA system used for simulations has $N = 1{,}024$ subcarriers and 16-QAM modulation. In a processing unit, six data blocks and one pilot block are considered. Each block consists of $M = 72$ complex modulated symbols. For the proposed method, the real factor of amplitude distortion is set to $\gamma = 1/2$ and the intervals of reserved symbols in the pilot block is set to $v = 6$. The complementary cumulative distribution function is employed as the measurement for the PAPR reduction, which is defined as the probability that the PAPR exceeds a given threshold, $PAPR_0$. To evaluate the BER performance, 6-tap rural channels are used.

Figure 3 shows a comparison of PAPR reduction performance for the proposed scheme and the conventional SC-FDMA. The threshold values for the proposed scheme for the number of iterations $K = 1, 2, 3$, and 4 are $[4.5]^T$, $[4.5, 5]^T$, $[4.5, 4.5, 5]^T$, and $[4.5, 4.5, 5, 5]^T$, respectively. It can be seen that the proposed method has a much better PAPR reduction performance than the conventional SC-FDMA scheme. As expected, the PAPR reduction performance of the proposed scheme improves as K increases. To achieve $\Pr(PAPR > PAPR_0) = 10^{-3}$, there is a gain of 1.5 dB for $K = 4$ as compared to the conventional SC-FDMA method.

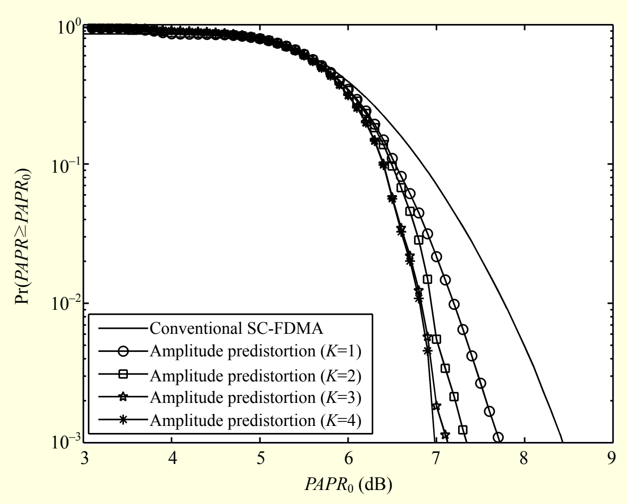

Fig. 3. Comparison of PAPR reduction performance of conventional and proposed schemes.

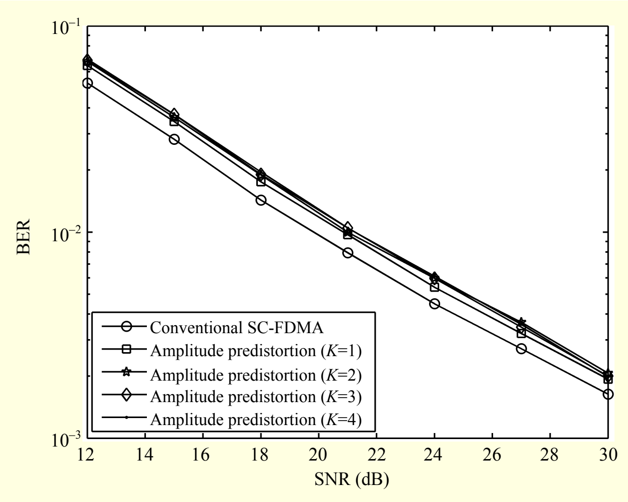

Fig. 4. Comparison of BER performance of conventional and proposed schemes for 6-tap rural channels.

Figure 4 shows a comparison of BER performance between the original SC-FDMA signal and the proposed scheme for 6-tap rural channels. It can be seen that the BER performances of the proposed scheme are almost the same for $K = 1, 2, 3$, and 4. Moreover, the proposed scheme suffers a slight loss in BER performance compared to that of the conventional SC-FDMA signal. The amplitude distortion will reduce the power of the distorted symbols, so there are possible error detections of the indices of the distorted symbols. However, as the value of K increases, so does the number of distorted symbols; hence, the computational complexity increases also. Thus, there is a trade-off between the PAPR reduction and the computational complexity as well as the BER performance.

VI. Conclusion

An amplitude predistortion–based PAPR reduction scheme is presented for SC-FDMA signals. Without transmitting side information, the proposed scheme can achieve good PAPR reduction performance with almost the same BER performance as the conventional SC-FDMA signals. It is expected that the proposed scheme will be very attractive for use in practical SC-FDMA systems, especially in those with high-order modulations.

References

[1] 3GPP TS 36.211, *Evolved Universal Terrestrial Radio Access (E-UTRA); Physical Channels and Modulation (Rel-12)*, Sept. 2014.

[2] G. Berardinelli et al., "OFDMA vs. SC-FDMA: Performance Comparison in Local Area IMT-A Scenarios," *IEEE Wireless Commun.*, vol. 15, no. 5, Oct. 2008, pp. 64–72.

[3] G. Huang, A. Nix, and S. Armour, "Impact of Radio Resource Allocation and Pulse Shaping on PAPR of SC-FDMA Signals," *Int. Symp. Pers., Indoor Mobile Radio Commun.*, Athens, Greece, Sept. 3–7, 2007, pp. 1–5.

[4] G. Wunder et al., "The PAPR Problem in OFDM Transmission: New Directions for a Long-Lasting Problem," *IEEE Signal Process. Mag.*, vol. 30, no. 6, Nov. 2013, pp. 130–144.

[5] S.B. Slimane, "Reducing the Peak-to-Average Power Ratio of OFDM Signals through Precoding," *IEEE Trans. Veh. Technol.*, vol. 56, no. 2, Mar. 2007, pp. 686–695.

[6] E. Hong et al., "Pilot-Aided Side Information Detection in SLM-Based OFDM Systems," *IEEE Trans. Wireless Commun.*, vol. 12, no. 7, July 2013, pp. 3140–3147.

[7] R. Salmanzadeh and B. Tazehkand, "A Modified Method Based on the Discrete Sliding Norm Transform to Reduce the PAPR in OFDM Systems," *ETRI J.*, vol. 36, no. 1, Feb. 2014, pp. 42–50.

[8] Y.-J. Cho, J.-S. No, and D.-J. Shin, "A New Low-Complexity PTS Scheme Based on Successive Local Search Using Sequences," *IEEE Commun. Lett.*, vol. 16, no. 9, Sept. 2012, pp. 1470–1473.

[9] J.-C. Chen and C.-P. Li, "Tone Reservation Using Near-Optimal Peak Reduction Tone Set Selection Algorithm for PAPR Reduction in OFDM Systems," *IEEE Signal Process. Lett.*, vol. 17, no. 11, Nov. 2010, pp. 933–936.

[10] P. Li et al., "Peak-to-Average Power Ratio of SC-FDMA Systems with Localized Subcarrier Mapping," *Global Mobile Congress*, Shanghai, China, Oct. 18–19, 2010, pp. 1–6.

[11] I. Baig, M. Ayaz, and V. Jeoti, "A SLM Based Localized SC-FDMA Uplink System with Reduced PAPR for LTE-A," *J. King Saud University - Eng. Sci.*, vol. 25, no. 2, July 2013, pp. 119–123.

[12] Y. Duan et al., "A New SLM Method with Feedback Searching for Uplink SC-FDMA System," *Int. Conf. Wireless Commun. Netw. Mobile Comput.*, Shanghai, China, Sept. 21–23, 2012, pp. 1–4.

[13] L. Wang et al., "A Time-Domain PTS without Side Information in SC-FDMA Systems," *Int. Conf. Wireless Commun., Netw., Mobile Comput.*, Wuhan, China, Sept. 23–25, 2011, pp. 1–4.

[14] A. Ahmed, M. Shokair, and E. Rabaie, "C42. PAPR Reduction for LFDMA Using a Reduced Complexity PTS Scheme," *National Radio Sci. Conf.*, Cairo, Egypt, Apr. 10–12, 2012, pp. 515–522.

[15] C. Meza, K. Lee, and K. Lee, "PAPR Reduction in SC-FDMA by Pulse Shaping Using Parametric Linear Combination Pulses," *IEEE Commun. Lett.*, vol. 16, no. 12, Dec. 2012, pp. 2008–2011.

[16] D.D. Falconer, "Linear Precoding of OFDMA Signals to Minimize their Instantaneous Power Variance," *IEEE Trans. Commun.*, vol. 59, no. 4, Apr. 2011, pp. 1154–1162.

[17] C.H.G. Yuen and F. Behrouz, "Analysis of the Optimum Precoder in SC-FDMA," *IEEE Trans. Wireless Commun.*, vol. 11, no. 11, Nov. 2012, pp. 4096–4107.

[18] J. Ji, G. Ren, and H. Zhang, "PAPR Reduction in Coded SC-FDMA Systems via Introducing Few Bit Errors," *IEEE Commun. Lett.*, vol. 18, no. 7, July 2014, pp. 1258–1261.

Yujie Xia received his BS degree in electronic engineering from Henan Normal University, Xinxiang, China, in 2001 and his MS degree in communication and information systems from Harbin Engineering University, China, in 2004. He received his PhD degree in communication and information systems from Xidian University, China, in 2014. Since 2004, He has been with the School of Physics and Electronic Information, Luoyang Normal University, China, where he is now an associate professor. His research interests are in the area of broadband wireless access, orthogonal frequency-division multiple access techniques, and communication signal processing.

Jinwei Ji received his BS degree in communications engineering from Hebei University of Technology, Tianjin, China, in 2009 and his PhD degree in communication and information systems from Xidian University, China, in 2015. Since 2015, He has been with the 54th Research Institute of China Electronics Technology Group Corporation, Shijiazhuang, China. His research interests include wireless communication and peak-to-average power ratio reduction for OFDM/SC-FDMA-based communication systems.

http://dx.doi.org/10.4218/etrij.15.0114.1194